Future projection of droughts in Morocco and potential impact on agriculture

Veysel Gumus[1,2,*], Nabil El Moçayd[3], Mehmet Seker[1], Mohammed Seaid[2]

[1] *Civil Engineering Department, Harran University, Sanliurfa, Turkey*
[2] *Department of Engineering, University of Durham, South Road, DH1 3LE, United Kingdom*
[3] *International Water Research Institute (IWRI) - Institute of Applied Physics (IAP), University Mohammed VI Polytechnic, Benguerir, Morocco*

Abstract

The present study evaluates the future drought hazard in Morocco using a Multi-Model Ensemble (MME) approach. First, the artificial neural network-based MME is constructed using the the General Circulation Models (GCMs) from the Climate Models Intercomparison Project phase 6 (CMIP6) which are most successful in representing the historical temperature and precipitation values. Next, the future changes in the precipitation, Potential EvapoTranspiration (PET) calculated using temperatures data, aridity index, and drought indices calculated via the Standardized Precipitation Evapotranspiration Index (SPEI) values were projected for the historical period 1980-2014, near future 2025-2050, mid future 2051-2075, and far future 2076-2100. The obtained results indicate that there will be a decrease in values of the precipitation and an increase in values of the PET, leading to an increase in aridity risk for Morocco. The future projections using the SPEI results show that the average index values will mostly be in the drought zone, indicating that the drought severity will increase. The spatial analysis of SPEI values in different regions of Morocco demonstrates that the northern part of the country has relatively more drought occurrences, and drought severity tends to increase with each passing period. The study also reveals that drought severity will significantly increase after 2050 in the Shared Socio-economic Pathways 5-8.5 (SSP5-8.5) scenario. The research concludes that the increase in drought severity will significantly impact Morocco's water resources, agriculture and food security among others.

Keywords. Climate change; Projections; CMIP6; Drought analysis; Artificial neural network

1 Introduction

Droughts are unfortunate natural disaster characterised by long periods of limited access to water, and has therefore non-negligible impact on humans (AghaKouchak et al., 2021), societies (D'Odorico et al., 2010) and food systems (Tardieu, 2020). Due to the diverse climate driving the region, northern Africa is strongly vulnerable to droughts and Morocco constitutes a case study in its point within this context (Le Page and Zribi, 2019). Throughout the past, the region has experienced

*Corresponding author: gumus@harran.edu.tr

many drought episodes that have led to disastrous social and economical disruptions (Esper et al., 2007). In a region where resilience is yet a challenging problem (Satour et al., 2021), some vital sectors for the development still suffer from the after-effects of these aforementioned events. This includes some direct sequels such as desertification (Benbrahim et al., 2004), landslide (Ivčević et al., 2020) and water shortage (El Moçayd et al., 2020) to name few, but also indirect ones such as poverty, hunger and social crisis (Anderson et al., 2021). The occurrence of droughts in Morocco is strictly linked to the high variability of precipitation and temperature. In fact, the climatic situation of the country is characterized by a strong temporal variability oscillating between sudden heavy precipitations and major episodes of drought. This situation renders water management in Morocco very challenging at different levels, especially to sustain agriculture (Doukkali, 2005). **In fact, as stated in (Elalaoui et al., 2021), the local economy in the country depends highly on agriculture as its contribution to local GDP can achieve 15%, compare the figure in page 200 of (Elalaoui et al., 2021)**. Moreover, many ongoing efforts by the local government intend to support this economy through launching several programs dedicated to support this vision, such as the Moroccan green project launched in 2008. Despite the economic benefits of such programs, this has led to increasing water demand as well (Ward and Pulido-Velazquez, 2008), increasing thus the vulnerability level of the agriculture in the country to droughts (Maggioni, 2015). Since the $1960s$, Morocco has actively pursued irrigation development resulting in approximately 1.5 million hectares, or 16% of the country's total arable land, now being irrigated. This is close to the estimated potential of 1.65 million hectares. The government has developed and managed two-thirds of this irrigated land through "irrigated perimeters" which encompass nine major regions covering nearly $900,000$ hectares and are equipped with extensive water collection and delivery systems. The remaining irrigated areas, totaling over 100 small-scale plots, are typically situated farther away from dams and rely more on local groundwater pumping. Despite comprising only 16% of arable land, irrigation contributes to 45% of the agricultural added value on average, which can rise to 70% in dry years, and accounts for 75% of agricultural exports (Kadi, 2002). Revenue per hectare from irrigated crops is four to eight times higher than that from rainfed crops (Tuel, 2020). In addition within this context, the drought remains a significant hurdle to sustaining irrigation and agricultural productivity. Given the proven vulnerability of Morocco to the drought (Driouech et al., 2021), it is crucial to closely analyze its various pathways under different climate change scenarios and understand the resulting impact on agriculture.

In practice, it is very difficult to quantify a drought event since many definitions according to the prism upon which it is analysed, are present in the literature (Wilhite and Glantz, 1985). Still, one can subdivide them into four different classes based on the socio-economical, agricultural, hydrological or meteorological impacts. Agricultural-based droughts are defined based on the intrinsic dynamics occurring between plants, soil and atmosphere, and they require data related to these systems such as soil moisture description, plant water demand and evapotranspiration deficit data (Liu et al., 2016). On the other hand, hydrological-based droughts are described based on the ability of the natural system to retain sufficient water for human use, and they are therefore based on water demand, hydrological description and water availability (Van Loon, 2015) among others. It should also be stressed that because of the large data requirements, which are not available within the environment of the study, the focus in the present study is brought to meteorological-based droughts. Generally, two indices are commonly used in the literature in the Mediterranean basin, namely the SPI (McKee et al., 1993) and the SPEI (Vicente-Serrano et al., 2010), and are also recommended by the World Meteorological Organisation (WMO) (Svoboda et al., 2012). Notice that the SPI defines droughts as long periods without rainfall supply, whereas the SPEI extends the definition also to the ability of natural systems to lose water through evaporation by introducing the water budget as

the deficit between precipitation and evaporation. Hence, based on these definitions, droughts vary alongside with climate parameters of variability in the country, particularly the precipitation and temperature.

The location of Morocco and its complex topography are all factors that strongly contribute to the high variability of the climate and some studies have confirmed that this variability has been consistent over a millennium time scale (Esper et al., 2007). The west region of the country is facing the Atlantic ocean in the extratropical region. Moisture availability is driven therefore by several large scale oscillations such as North Atlantic Oscillation (NAO) (Knippertz et al., 2003) for large time scale, and Madden Julian Oscillation (MJO) (Chaqdid et al., 2023) in moderate time scale. On the north-eastern part of Morocco facing the Mediterranean sea, a water body surrounded by three continents (Africa, Europe and Asia) with a small connection to the Atlantic ocean of approximately 14 km at the Strait of Gibraltar. This puts Morocco under the excitation of the Mediterranean Oscillation (MO), which is characterised by a strong and robust cyclonic activities over the sea that sustain a strong wind flow bringing dry and hot air from the sahara region towards the country (Filahi et al., 2016). Note that these numerous excitations translate into complex weather in the country, driving most of the time the climate to extreme conditions (Filahi et al., 2016; Khomsi et al., 2016). Furthermore, the Mediterranean region is a host for considerable climate change impact (Tuel and Eltahir, 2020). Thus, Morocco is particularly vulnerable to future changes, especially regarding water management. It is worth mentioning that with projected increase in temperature and decrease in precipitation, the country is more likely to receive little water compared to the present situation. This will impact different essential components of the hydrological system which have major contributions to the agricultural economy such as river stream flows (El Moçayd et al., 2020), snow coverage (Tuel et al., 2022) and soil moisture among others. In addition, with the growing number of drought episodes, this situation could be considerably worse in future scenarios. In general, future projections are assessed using imperfect models that hardly capture all the complexity expressed in the local climate. This is particularly true for Morocco where the uncertainty of climate simulations is further increased as observational ground data in the region are sparse and historical records are not long enough. This may explain why modelling the extreme climate in Morocco is still challenging and has received little attention compared to average climatology.

Although many studies have addressed the drought modelling in the region, still many challenges remain unresolved. One of the main limitations in these studies is the scarcity of data, especially those required to address extreme weather conditions. For this purpose, (Ezzine et al., 2014) introduced a new drought index based on open data referred to by Standardized Water Index (SWI). The obtained results exhibit good agreement between the introduced SWI and the SPI and highlighted the limitations expressed by the use of short time series. The climate variability and important seasonality are also important hurdles regarding the drought monitoring in the region as reported in (Fniguire et al., 2017). Furthermore, the climate change impact on drought occurrences has not received enough attention because of the challenges aforementioned. For example (Elkharrim and Bahi, 2015) evaluated future projections of drought in the Bouregreg basin using a statistical downscaling model from HadCM3 outputs in order to predict future scenarios. It should also be stressed that based on recent works, statistical downscaling may suffer from some limitations. In addition to the limitation presented by the small size of historical records, all the General Circulation Models (GCMs) fail to correctly capture all the physical mechanisms responsible for the observed climatic variability in Morocco (Tuel et al., 2021). Accordingly, the choice of the GCMs for downscaling should be performed carefully, mainly for extreme events whose physical drivers are profoundly different.

In the present study, based on the development of new station-based historical records in the

region and with the development of CMIP6 experiments whose description takes into account different concentration pathways and different socio-economic projections accurately compared to the previous CMIP3 or CMIP5, we demonstrate that evaluations of drought and its future projections are possible. This issue is addressed in this study using an Artificial Neural Network (ANN) based statistical downscaling together with a careful choice of the GCM description. First, climate variables such as temperature and precipitation are fully described for all the observation stations, then mapping of these variables over the country is performed using a spatial interpolation. Moreover, the evaluation of droughts is carried out using the SPEI in order to take into account the balance between water availability and potential loss through evaporation. Next, future projections of droughts following mitigation and business-as-usual scenarios are evaluated. Finally, as agriculture is the main vital economical sector vulnerable to climate change in the country, future projections of the SPEI during the growing seasons are discussed and the potential impact on the main crops is also highlighted. The remainder of this paper is organized as follows: Section 2 describes the study area, including the observing stations and CMIP6 GCMs used in the drought analysis. Next, in Section 3, we describe the procedure used in this study for statistical downscaling and the SPEI method. Section 4 evaluates the historical and possible future drought patterns with those results obtained by projecting values of the precipitation, PET and Aridity Index in the considered region. This section also covers the relationship between the drought and agricultural production. Discussions on differences and agreements of the results obtained for the region with previous studies are presented in Section 5. Finally, Section 6 summarizes the paper with concluding remarks.

2 Study area and data

Morocco, a substantial and expansive nation situated in the northwestern region of the african continent (see Figure 1), experiences a localized climate impacted by the interaction of many large-scale oscillations with a complex topography. The country's western coastline, which faces the vast Atlantic ocean, is subject to the influence of the North Atlantic Oscillation (NAO) (Knippertz et al., 2003), a climatic phenomenon that exerts a profound effect on the availability of moisture and precipitation patterns across Morocco. In addition, the country's northeastern region is influenced by the intricate dynamics of the Mediterranean sea, particularly in future projections, where the interplay between land and sea is pivotal in rendering the area highly susceptible to the impacts of climate change (Tuel and Eltahir, 2020). Recent research has further unveiled additional large-scale phenomena responsible for regulating the region's climate variability such as the Madden-Julian Oscillation (MJO) (Gadouali et al., 2020; Chaqdid et al., 2023). Furthermore, the country's topography poses additional complexities, with the towering Atlas and Rif mountains significantly shaping the temperature and precipitation patterns that characterize Morocco's climate.

The implementation of measured data as opposed to reanalysis data in the context of statistical downscaling is known to enhance the predictive performance of the models (Manzanas et al., 2015). To this end, the present study draws upon observation stations in Morocco provided by the national meteorological agency known by the Direction Générale de la Météo (DGM), undertakes regular measurements. In Table 1, we summarize the characteristics associated with these stations including their ID and geographical coordinates and long-term averaged values for minimum daily temperature (T_{min}), maximum temperature (T_{max}) and daily precipitation (Prep). In order to carry out statistical downscaling, daily measurements recorded at these stations were first transformed into monthly values. In particularly, monthly averaged minimum and maximum temperatures were calculated based on the monthly averages of daily minimum and maximum temperatures (° C)

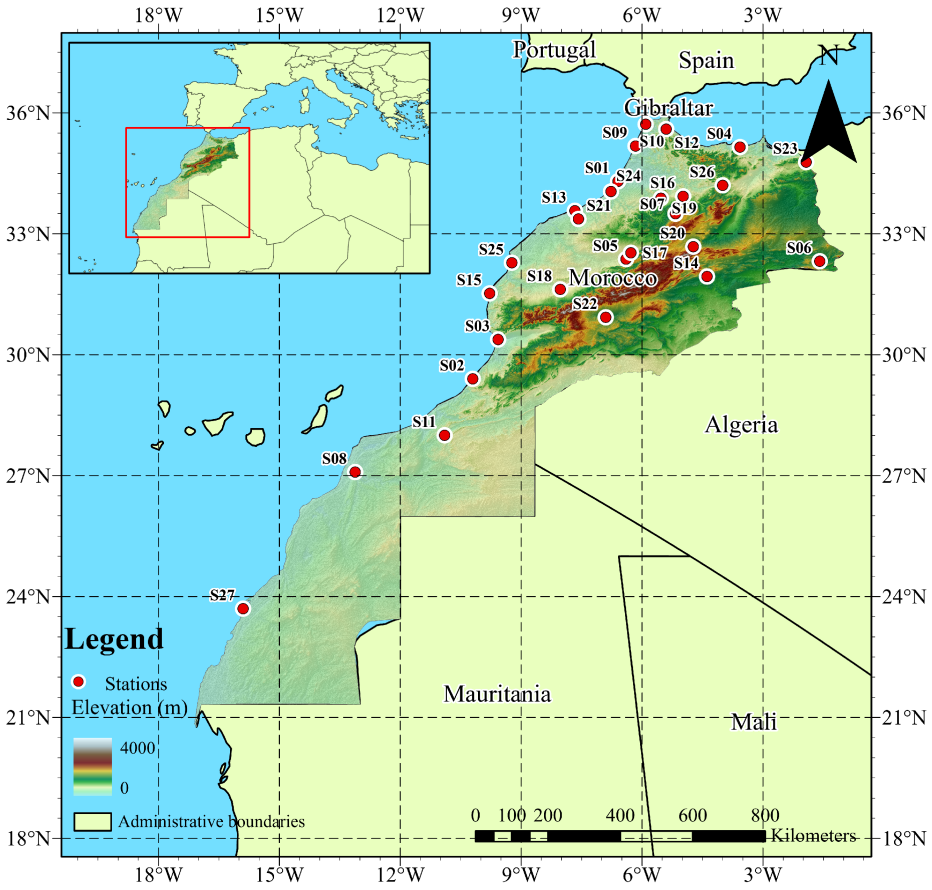

Figure 1: Study area including Morocco's geographical regions considered in the present work.

whereas precipitation values were derived from the average of daily measurements (mm/day). In these stations, data between 1980 and 2014 were used and among these data, only one station has 8% missing data, while this rate is 1% or less in other stations. Notice that the missing data were completed through the linear regression method and the neighbouring stations' data. Thus, a time series was obtained for the years 1980-2014 for all stations to be used in the statistical downscaling.

In the current work, temperature and precipitation data obtained from the Multi Model Ensemble created by (Gumus et al., 2023) for Morocco are used in the assessment of drought. In the study of (Gumus et al., 2023), the CMIP6's 15 GCMs are selected to analyse historical data of monthly mean daily precipitation, monthly mean maximum temperature and monthly mean minimum temperature. These GCMs are available from the Earth System Grid Federation[1] (ESGF). The institutes, variable labels, horizontal and vertical resolutions of the GCMs used in our study are listed in Table 2. In order to establish a common working concept between the models, careful analysis has been carried out to ensure they have the same variance (r1i1p1f1). However, due to the lack of past or future data for variables selected as inputs to ANN-based downscaling, different variants have been used in the four GCMs. Furthermore, since the considered models have different horizontal and vertical resolutions, the latitude-longitude location of the observation stations have been interpolated to

[1]https://esgf-node.llnl.gov/ search/cmip6

Table 1: Geographical coordinates and mean values of used climate variables of stations considered in this study.

Station ID	Station Name	Longutude (°)	Latitude (°)	T_{min} (° C)	T_{max} (° C)	Prep (mm/day)
S01	KENITRA	-6.60	34.30	13.25	23.12	1.534
S02	SIDI IFNI	-10.20	29.40	16.78	21.89	0.412
S03	AGADIR	-9.57	30.38	14.34	24.09	0.717
S04	ALHOCEIMA	-3.57	35.15	13.93	22.27	0.875
S05	BENI MELLAL	-6.40	32.37	11.24	26.92	0.985
S06	BOUARFA	-1.59	32.32	11.98	24.74	0.437
S07	IFRANE	-5.17	33.50	6.21	18.16	2.648
S08	LAAYOUNE	-13.12	27.09	15.97	26.43	0.155
S09	LARACHE	-6.16	35.18	13.62	22.31	1.881
S10	TANGIER	-5.91	35.72	13.69	22.48	1.886
S11	TANTAN	-10.90	28.00	15.55	23.62	0.298
S12	TETOUAN	-5.40	35.60	14.74	22.72	1.852
S13	CASABLANCA (ANFA)	-7.67	33.57	14.50	21.94	1.104
S14	ERRACHIDIA	-4.39	31.94	13.19	26.39	0.348
S15	ESSAOUIRA	-9.78	31.52	15.11	20.43	0.882
S16	FES	-4.98	33.93	10.22	24.16	1.329
S17	KASBAT TADLA	-6.28	32.53	12.02	26.88	1.011
S18	MARRAKESH	-8.03	31.62	13.46	27.26	0.609
S19	MEKNES	-5.53	33.88	11.39	23.91	1.335
S20	MIDELT	-4.73	32.68	8.45	21.78	0.479
S21	CASABLANCA (AIRPORT)	-7.58	33.37	11.85	24.01	0.845
S22	OUARZAZATE	-6.90	30.93	12.25	26.99	0.333
S23	OUJDA	-1.93	34.78	10.85	24.31	0.734
S24	RABAT SALE	-6.77	34.05	12.74	22.49	1.390
S25	SAFI	-9.23	32.28	13.83	23.60	1.015
S26	TAZA	-4.00	34.20	12.79	24.62	1.518
S27	DAKHLA	-15.90	23.70	17.12	24.12	0.078

establish a common position for both observations and models. Finally, cereal production in Morocco is obtained from the Food and Agriculture Organization (FAO) available on the website FAOSTAT. This database provides different information on crop production on a country level.

3 Methods for statistical downscaling and SPEI

The assessment of possible future droughts in Morocco is primarily based on the future projection of precipitation and temperature in the country. For this purpose, daily observed climate data are converted to monthly averaged values. Next, spatial interpolation using a bi-linear reconstruction is carried out to define the 21 parameters of the GCMs as potential predictors according to the corresponding geographical coordinates of the observation stations. **The main reason for using the bilinear interpolation lies in the fact that this method can transform the data from a coarser resolution to a finer resolution without affecting the climate signal (Ahmed et al., 2020). Consequently, re-gridding of GCMs does not significantly affect their**

Table 2: The CMIP6 GCMs used for the climate projection.

No	Name CMIP6 model	Country	Resolution (° lon ×° lat)	Variant label	Key reference
1	ACCESS-CM2	Australia	1.9° × 1.3°	r1i1p1f1	(Bi et al., 2013)
2	CanESM5	Canada	2.8° × 2.8°	r1i1p1f1	(Swart et al., 2019)
3	CanESM5-CanOE	Canada	2.8° × 2.8°	r1i1p2f1	(Swart et al., 2019)
4	CNRM-CM6-1-HR	France	0.5° × 0.5°	r1i1p1f2	(Voldoire et al., 2019)
5	CNRM-ESM2-1	France	1.4° × 1.4°	r1i1p1f3	(Séférian et al., 2019)
6	EC-Earth3-Veg	Europe	0.7° × 0.7°	r1i1p1f1	(Wyser et al., 2020)
7	FGOALS-g3	China	2.0° × 2.3°	r1i1p1f1	(Li et al., 2020b)
8	GFDL-ESM4	USA	1.25° × 1.0°	r1i1p1f1	(Dunne et al., 2020)
9	GISS-E2-1-G	USA	2.5° × 2.0°	r1i1p1f2	(Kelley et al., 2020)
10	INM-CM5-0	Russia	2.0° × 1.5°	r1i1p1f1	(Kulyamin and Volodin, 2018)
11	IPSL-CM6A-LR	France	2.50° × 1.26°	r1i1p1f1	(Boucher et al., 2020)
12	MIROC6	Japan	1.41° × 1.41°	r1i1p1f1	(Tatebe et al., 2019)
13	MPI-ESM1-2-HR	Germany	0.937° × 0.937°	r1i1p1f1	(Gutjahr et al., 2019)
14	MRI-ESM2-0	Japan	1.125° × 1.125°	r1i1p1f1	(Yukimoto et al., 2019)
15	NESM3	China	1.9° × 1.9°	r1i1p1f1	(Cao et al., 2018)

Table 3: Classification of the SPEI.

SPEI values	Drought class
$-1.0 < \text{SPEI} \leq 0$	Mild Drought (MD)
$-1.5 < \text{SPEI} \leq -1.0$	Moderate Drought (MoD)
$-2.0 < \text{SPEI} \leq -1.5$	Severe Drought (SD)
$-2.0 \geq \text{SPEI}$	Extreme Drought (ED)

performance (Pour et al., 2018). It should also be stressed that other interpolation procedures can also be used in our study without major conceptual modifications. These potential predictors are air temperature, relative humidity and geopotential height for five pressure levels (*i.e.* 200, 300, 500, 700 and 850), sea level air pressure, surface air pressure, precipitation, minimum temperature T_{min}, maximum temperature T_{max}, and mean near-surface temperature. Then, five of the predictors with the highest correlation with the observation data are then determined as predictors, and an artificial neural network model is constructed to predict the observation data. After determining the ANN-based model that best predicts the observation data according to the criteria detailed in (Gumus et al., 2023), the Multi-Model Ensemble (MME) is created using the most successful models. Finally, future precipitation and temperature values for two different Shared Socioeconomic Pathways (SSP2-4.5 and SSP5-8.5) scenarios are calculated for each station using the input parameters used to predict the observation data and the ANN model. Details of this procedure can be found in (Gumus et al., 2023) and will not be repeated here. Next, the precipitation and temperature values obtained with this approach are used for the estimation of drought indices.

Based on the impact of climate change on the variation of temperature, the evaporation process

may have important effects on the water availability and this contribution needs to be emphasized. For this reason, the Standardized Precipitation Evapotranspiration Index (SPEI) method is implemented here using values of the precipitation and potential evapotranspiration (PET) to estimate the drought indices. Future projections of the PET are estimated using temperature data and their projections under climate change scenarios. **The SPEI method, first introduced by (Vicente-Serrano et al., 2010) and later revisited by (Begueria et al., 2014), calculates the difference (D) between the monthly precipitation (P) and the potential evapotranspiration (PET) for each month. The resulting D values are then transformed to a standard normal distribution by fitting them to a log-logistic distribution, yielding the SPEI values. Although there are studies suggesting the use of different distributions for the SPEI method such as (Wang et al., 2019; Stagge et al., 2015), the log-logistic distribution has been shown to be very effective in several key studies including the original works by (Vicente-Serrano et al., 2010; Begueria et al., 2014) and recent research by (Lee et al., 2024). Needless to mention that given the change in data structure with the addition of historical and projection data, this study adopts the log-logistic distribution as used in the classical SPEI method for consistency and effectiveness.** The drought classification used in this study is outlined in Table 3, and further details on the method can be found in the abovementioned references.

It is worth noting that the calculation of PET values, which is necessary for computing the D in conjunction with precipitation, can significantly impact the results. Although the Penman-Monteith method produces the most accurate PET values, the necessary data required for this study is unavailable. Therefore, the Hargreaves-Samani method is used instead. This method produces results comparable to the Penman-Monteith method (Begueria et al., 2014; Ortiz-Gómez et al., 2022). It should also be stressed that since measured data to be used in the calculation of PET values using the Penman-Monteith method are not available for the considered case study, we opt for the Hargreaves-Samani approach in this study. The use of SPEI is preferred (especially against SPI), as the the study area is located in the mid latitude. Accordingly, the precipitation deficit may not be sufficient to fully describe the drought conditions accurately (Li et al., 2020a).

4 Results

In this section, the Multi-Model Ensemble (MME) generation process is briefly described first and then, changes in the calculated SPEI values of the parameters which are important for the drought according to different scenarios are evaluated temporally and spatially. For the results presented in this section, the analysis of GCMs and artificial neural network modelling are carried out using Matlab software whereas the R tools (SPEI package) were used for the calculation of drought index values.

4.1 Projection of climatic data

Following the methodology presented in section 3, for each GCM description an ANN model is constructed and climate variables are estimated. The performance of each model to predict T_{min}, T_{max} and precipitation is evaluated using the approach detailed in (Seker and Gumus, 2022) for statistical downscaling. Next, the MMEs are generated using the models that are most successful in representing the historical values of each parameter. Accordingly, EC-Earth3-Veg, NESM3 and

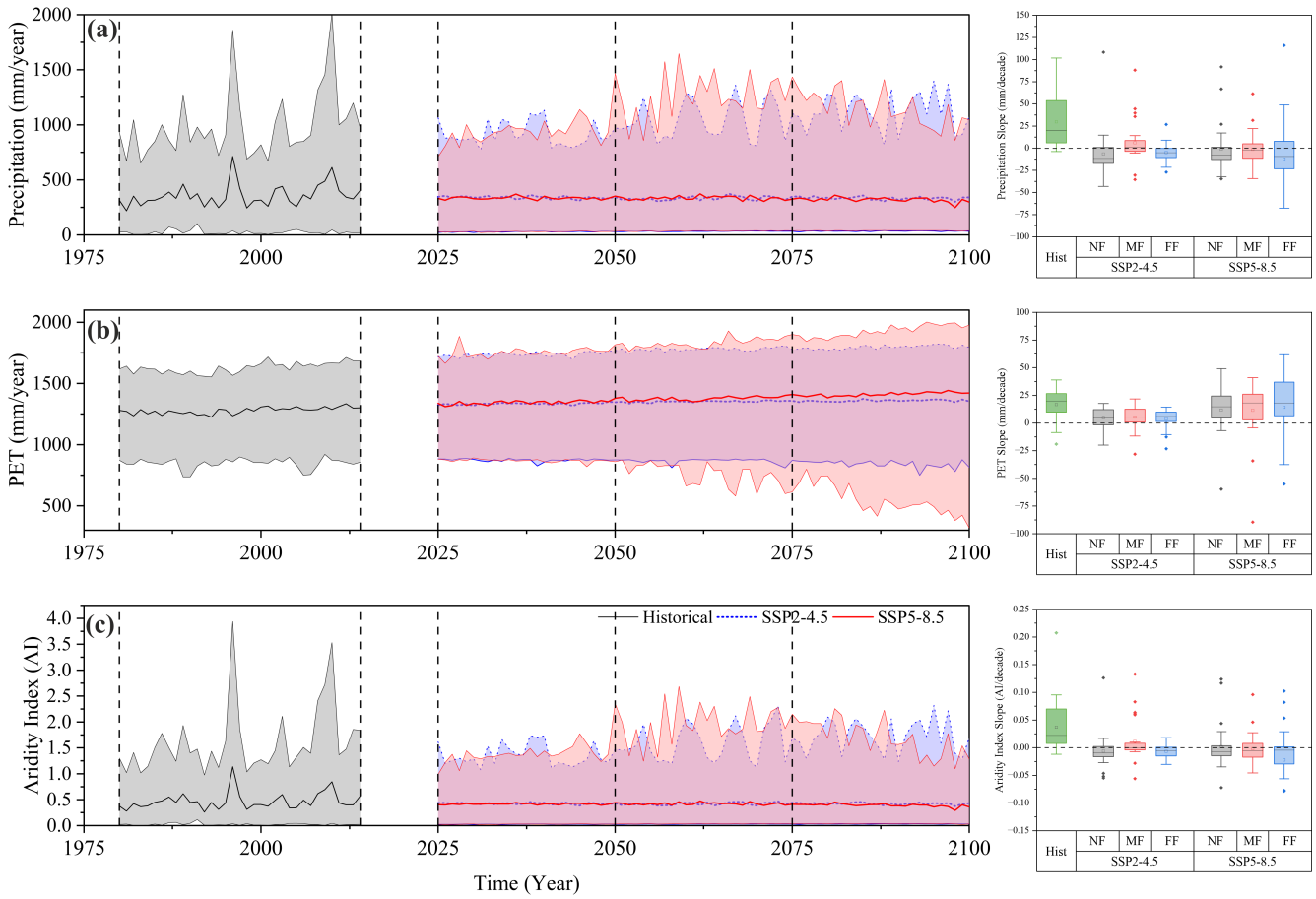

Figure 2: Temporal variation of Precipitation, PET and Aridity Index values along with box plots of their trend slopes.

MPI-ESM1-2-HR are used for T_{min}, EC-Earth3-Veg, NESM3, CanESM5-CanOE and MPI-ESM1-2-HR for T_{max}, and MIROC6, CanESM5-CanOE, IPSL-CM6A-LR, INM-CM5-0 and NESM3 for the precipitation. Using these MMEs, projections of future temperature and precipitation values are calculated. The results are obtained for the historical period 1980-2014, Near Future (NF) 2025-2050, Mid Future (MF) 2051-2075 and Far Future (FF) 2076-2100.

Next, values of the PET and aridity index are estimated following the method described in section 3 using the predicted values of T_{min}, T_{max} and precipitation for different scenarios. The temporal changes of these values are presented in Figure 2, and spatial changes are displayed in Figure 3. The distribution of precipitation between 1980 and 2014 shows that there was a peak precipitation in 1996 and 2010, and the averaged precipitation was 360 mm/year when all stations are considered (see Figure 2 (a)). It is also clear that precipitation has shown a slightly increasing trend during this period and it has an increasing trend of 30 mm/decade on average at the considered stations. However, it is predicted that the trend of changes in the precipitation according to future scenarios will turn into a decreasing trend in NF. Following the pessimistic SSP5-8.5 scenario, the decrease slope in FF may achieve -12 mm/decade. The PET values shown in Figure 2 (b) are calculated depending on the temperature values. The distribution of PET values calculated from the averaged stations 1280 mm/year between 1980 and 2014 and it varies between 750 and 1600 mm/year. Note that on average, the rate of PET slope for this period is 16 mm/decade, but it is projected to

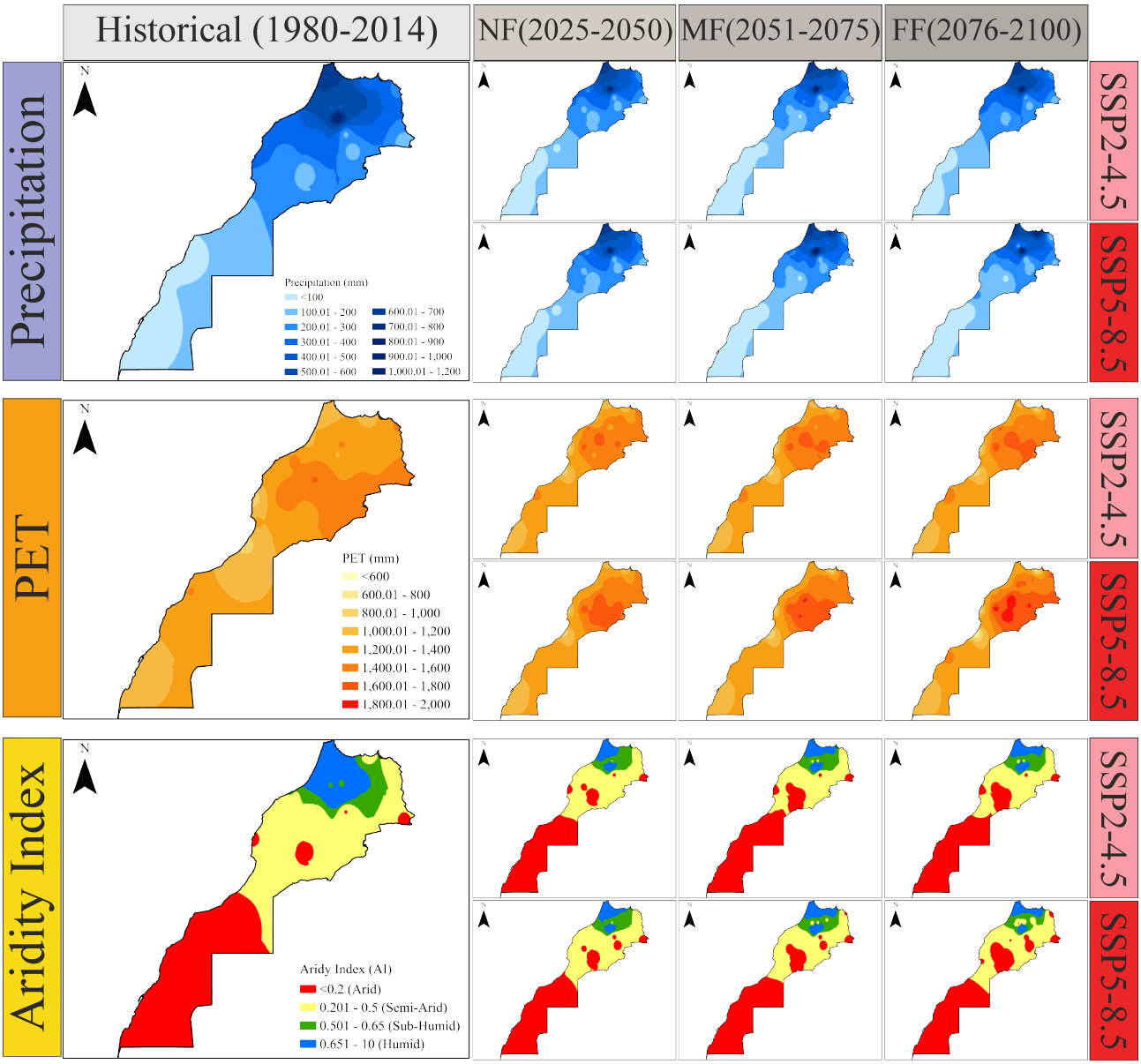

Figure 3: Spatial variation of Precipitation, PET and Aridity Index values.

decrease to 4.5 mm/decade by 2100 under the SSP2-4.5 scenario.

On the other hand, following the SSP5-8.5 scenario, the rate of change for the PET may achieve 11.7, 11.5 and 14.1 mm/decade for NF, MD and FF, respectively. Figure 2 (c) depicts the temporal changes and slopes of Aridity Index ($AI = \frac{P}{PET}$) calculated based on values of the precipitation and PET. The United Nations Environment Programme (UNEP) and the world atlas of desertification (Middleton and Thomas, 1992) employ the AI to delineate arid regions (with an AI<0.65) and to categorise them into distinct subtypes: arid (AI<0.2), semi-arid ($0.2 \leq AI < 0.5$), and dry sub-humid ($0.5 \leq AI < 0.65$) regions, as outlined by (Yu et al., 2022). According to Figure 2, the AI values across Morocco have an average of 0.47 (median 0.43) and an increasing slope of 0.03/decade. However, according to both scenarios, it is evident that the AI values will decrease from NF to FF, and the aridity structure of many regions may change. Following the SSP5-8.5 scenario, the decrease rate of the aridity index may achieve -0.02 in the FF. Overall, Morocco is likely to face a considerable risk

Table 4: Changes in the coverage area of aridity classes between historical and future periods in Morocco.

Class	**Hist**	**SSP2-4.5**			**SSP5-8.5**		
		NF	**MF**	**FF**	**NF**	**MF**	**FF**
Arid	42%	48%	53%	53%	49%	51%	53%
Semi-Arid	41%	38%	33%	33%	38%	35%	37%
Sub-Humid	7%	8%	8%	8%	8%	7%	6%
Humid	10%	6%	6%	7%	6%	7%	5%

of aridity resulting from the important decrease of precipitation and the increase in temperature.

Figure 3 presents the spatial distribution in values of precipitation, PET and Aridity Index in the historical and future for the SSP2-4.5 and SSP5-8.5 scenarios. The precipitation pattern exhibits a high spatial variability with an important gradient of distribution with very wet conditions in the north and a dry situation in the south. It is recognized that the precipitation values calculated with the MME will decrease for both scenarios, but the amount of decrease will be higher in the FF period of SSP5-8.5. Especially in the Sahara region located in the south of the country, it is noted that the region with low rainfall will move towards the north of the country. The change in averaged values of the precipitation calculated using the distribution of precipitation in the maps also supports the results of spatial patterns. According to the SSP2-4.5 scenario, the averaged annual total precipitation value calculated as 295 mm between 1980-2014 is estimated to be 273, 260 and 259 mm in the NF, MF and FF periods, respectively. Notice that the averaged annual total precipitation is calculated as 267, 256 and 245 mm in NF, MF and FF periods according to the SSP5-8.5 scenario. Regarding both scenarios, it is evaluated that the precipitation values would decrease to 245 mm at the end of the century in the pessimistic scenario; in other words, an average decrease of 17% would occur.

The distribution of PET values indicates that calculated annual PET values in the country between 1980 and 2014 were 1000-1600 mm, while the country average was 1286 mm. As for the future PET values, it is clearly understood that they increase as time advances, especially in the northern region of the country. Therefore, assuming the estimation of the SSP5-8.5 scenario, approximately 26% of the country will exceed 1600 mm, and the country's average PET value will reach 1410 mm in that period. Climate change impact on the precipitation and PET values will significantly alter the country's aridity structure in the future. This change is revealed by the spatial distribution of aridity values which indicates a substantial departure from the past conditions. It is recognised from Figure 3 that the country's southern region will be arid, and the northern region will be semi-arid in general except for a part of the northern region in the period 1980-2014. The temporal trend values in both scenarios indicate a decrease in the AI values, with the sub-humid and humid regions in the north of the country shrinking and the arid region expanding towards the north. The aerial distribution of aridity classes in the country between 2025-2100 is listed in Table 4. In the historical, the areas classified as Arid, Semi-Arid, Sub-Humid and Humid constitutes 42%, 41%, 7% and 10% of the country, respectively. It should be stressed that both scenarios predict further spatial deployment of the aridity class in the country in the future as 49% (in NF) and 53% (in FF) of the country is likely to be considered as an arid area. This will ultimately impact the region considered as sub-humid and humid areas since only 17% in NF and 11% in FF of the country

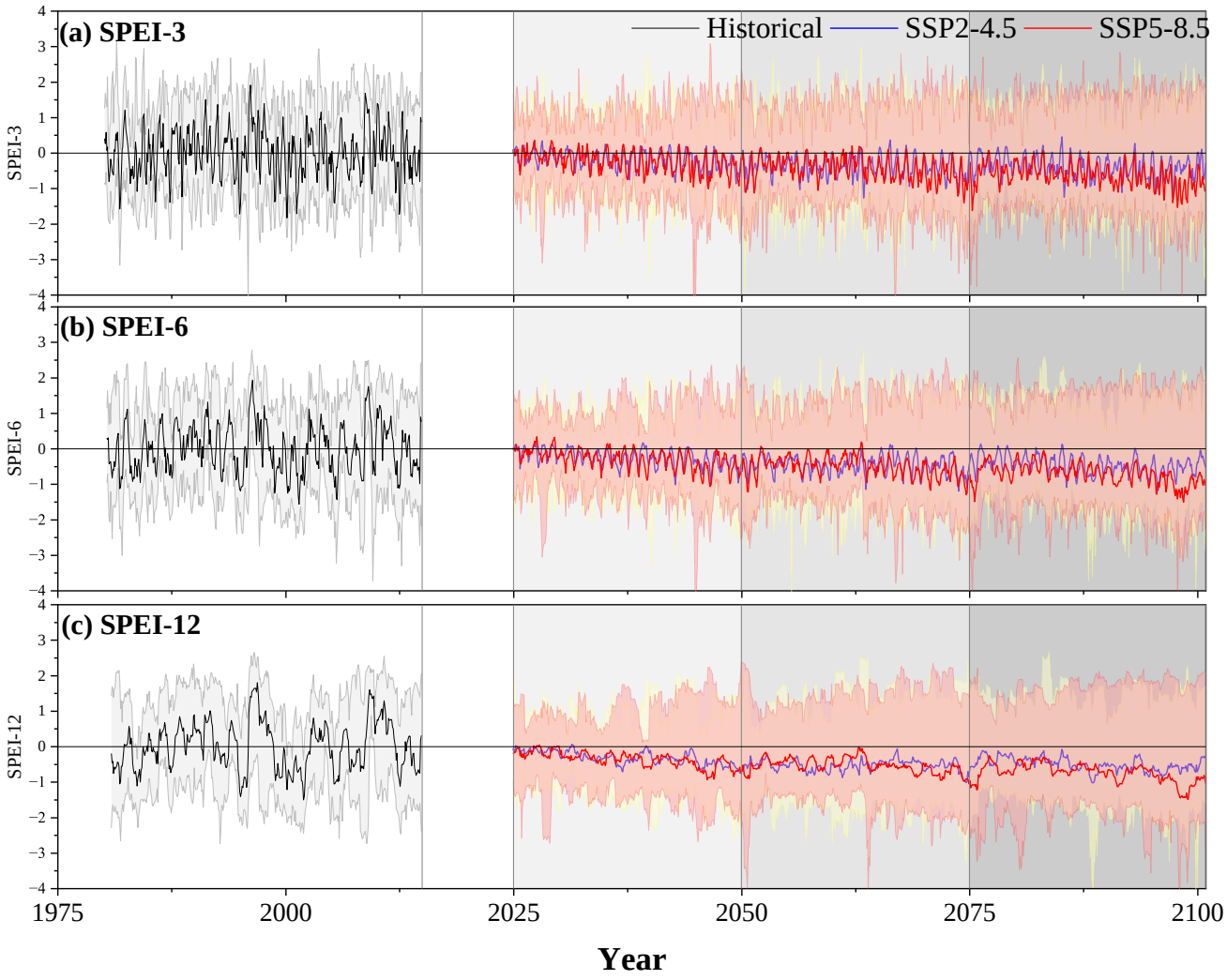

Figure 4: Temporal distribution of SPEI values for 3 (a), 6 (b) and 12 (c) month scale.

is likely to fit this class. Hence, under both scenarios, climate change is going to expand aridity in the country enhancing thus further water stress and other related agricultural problems such as saltwater intrusion and soil degradation among others.

4.2 Temporal variation of SPEI

The SPEI values are calculated for 3, 6 and 12 months time scales using the precipitation and PET values. Figure 4 displays the temporal distribution, where the fills represent the ranges of SPEI values at the stations, and the lines indicate the mean SPEI values. For comparison of the SPEI values calculated in this section for different periods, the SPEI values are calculated separately for four different time series (namely 1980-2014, 1980-2050, 1980-2075 and 1980-2100). Then, the corresponding period is extracted from these time series and added to the previous time series. For example, the SPEI values calculated for 1980-2014 are created only from observed values, and then 2025-2050 are extracted from the index values calculated for 1980-2050 and added. A similar process is repeated for 2050-2075 and 2076-2100. This is mainly because if an index is obtained from the

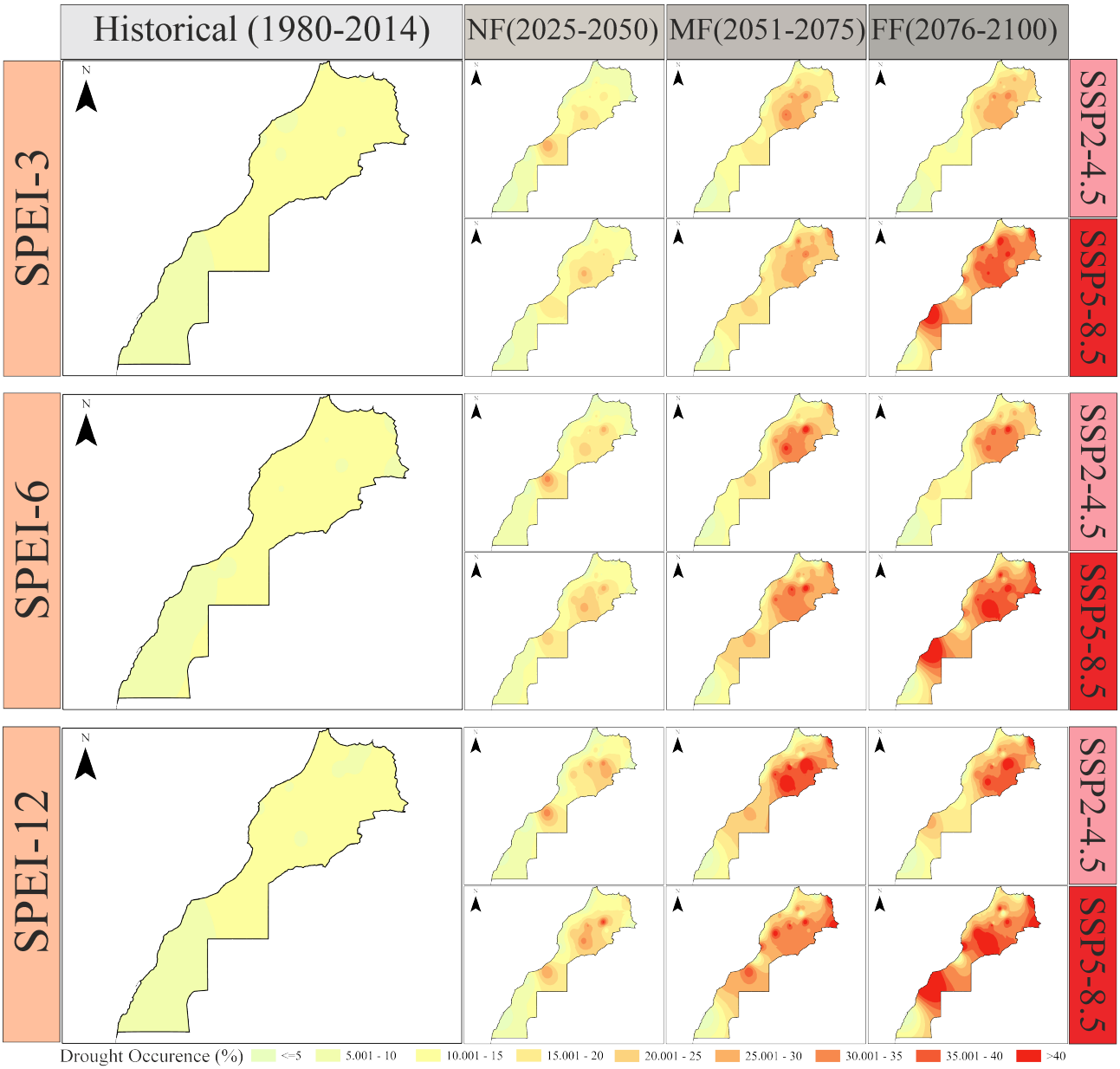

Figure 5: Spatial variation of SPEI values for the moderate class.

time series between 1980-2100, the values between 1980-2014 would completely change since the averaged precipitation and PET values would change. However, in this case, the existing situation would have been evaluated as of the end of 2100, and it would not be reliable to analyse changes in the current drought situation. Using this approach, since the index status at the end of each period (*e.g.* NF) analyzed will be independent of the next one, it will be possible to compare how the change will be compared to the periods before that period.

Concerning the SPEI3 values in Figure 4 (a), it is clear that the averaged index values for the historical are similar for the occurrence of drought (SPEI<0) and wet (SPEI>0). In addition, the slope value in historical is also determined to be in a decreasing trend and very low (slope $= -2.13 \times 10^{-5}$ per year). However, considering future droughts, although the distribution of minimum and maximum index values calculated at the stations are similar to the past period, the averaged values are quite different. It is seen that the averaged values are mostly in the drought zone

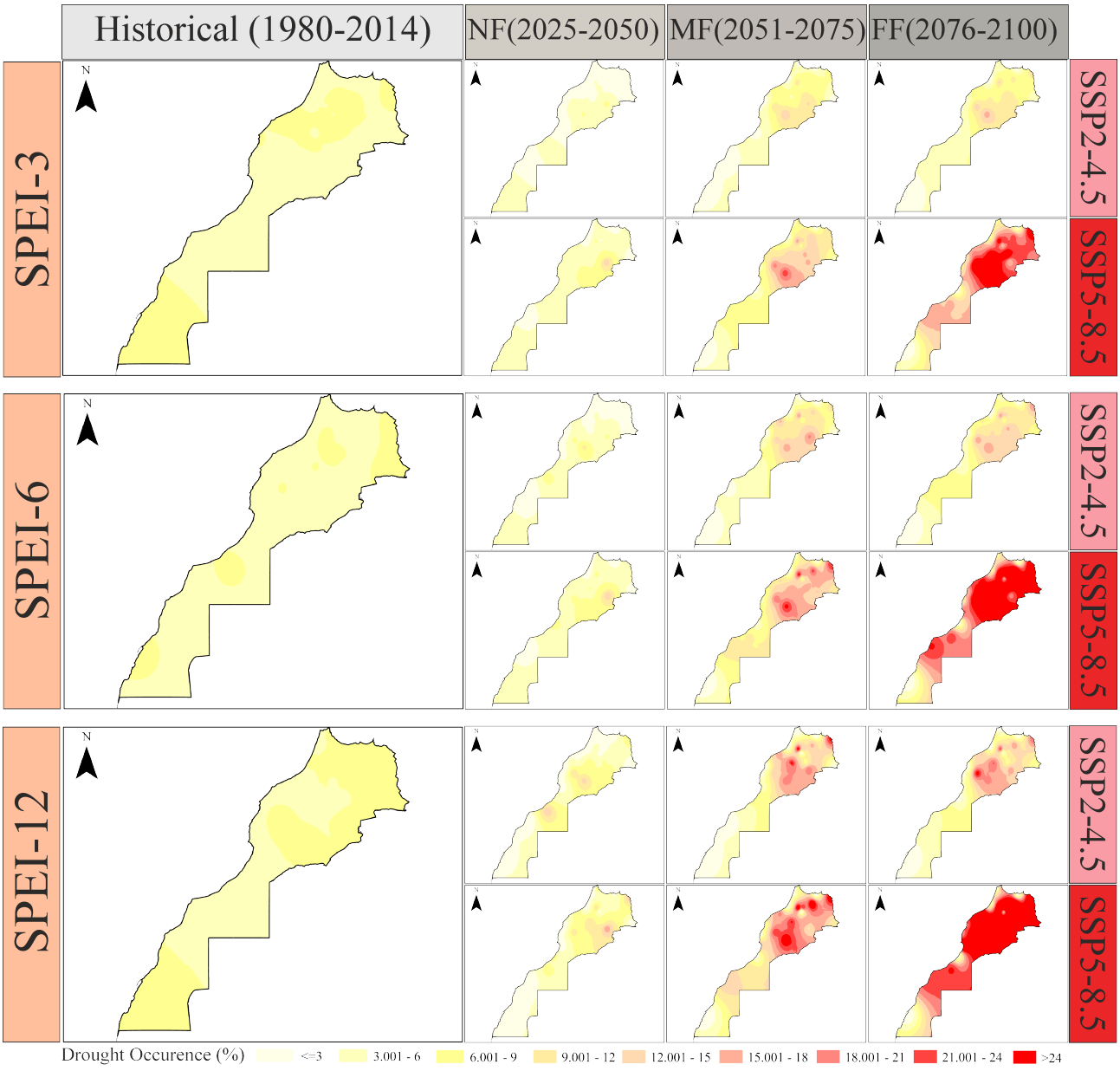

Figure 6: Spatial variation of SPEI values for severe and the extreme class.

(SPEI≤ 0) in the future projection, and the slope of the index values also increases. For example, in the SSP2-4.5 scenario, the slope value is approximately -3.5×10^{-4} per year in NF and FF and -1.5×10^{-4} per year in MF, while the SSP5-8.5 scenario is -6.1×10^{-4}, -6.5×10^{-4} and -6.8×10^{-4} per year in NF, MF and FF, respectively. In addition, it indicates that the negative slope increases with each passing period, *i.e.* drought severity tends to increase. A similar situation is also observed in the SPEI-6 and SPEI-12 scenarios. Nonetheless, the slope of historical index values in these time scales is positive (approximately 1.2×10^{-4} per year), this slope turns negative in the future projections and it reaches -7.5×10^{-4} per year in the SSP5-8.5 scenario.

4.3 Spatial variation of SPEI

Given the high spatial variability of climate in Morocco, it is important to analyse the spatial distribution of drought indices in the country. For this purpose, the percentages of occurrence of drought classes according to the three periods and two different scenarios are analysed. The percentages of occurrence in MD ($-1 \leq$ SPEI < -1.5) and SD and ED (SPEI ≤ -1.5) for 3, 6 and 12 months SPEI values are shown respectively, in Figure 5 and Figure 6 according to the classifications given in Table 3. Here, Figure 5 confirms that the percentage of MD occurrence ranges from 7% to 15% in all three time scales (the occurrence here is calculated based on the number of times on which the SPEI is under the threshold defined in Table 3). The southern part of the country generally exhibits lower drought, while the northern part has relatively more MD drought occurrences. For the SPEI-3 scenario in NF, the percentage of MD occurrence in the northern and the eastern regions starts to become more pronounced, and especially for the SSP5-8.5 scenario, the percentage of MD drought occurrence in NF reaches a value close to 50%. Note that as the drought time scale increases, the percentage of drought occurrence increases significantly in the MF and FF periods of the SSP2-4.5 scenario. It is worth mentioning that the most significant situation is observed in the SPEI12. At this time scale, the percentage of MD occurrence in almost the entire region of the country, except the Sahara region, is around 50%, and the percentage of drought occurrence in this class increases almost tenfold after 2050 compared to historical.

Figure 6 presents percentages of the occurrence of droughts above SD which are more severe and therefore can have multiple negative impacts on hydrological and agricultural activities. It is also clear that between 1980 and 2020, the percentage of occurrence of these drought classes varies between 4% and 8%. The percentage of occurrence of these drought classes increases in the NF, but significant increases are observed after 2050 following the SSP5-8.5 scenario. According to the SSP2-4.5 scenario for the MF and FF periods, drought occurrence in the northern and eastern regions for the SPEI6 and SPEI12 scenarios increases and locally reaches values of 20%. However, for the SSP5-8.5 scenario, drought occurrence is above 25% in those same locations according to the SPEI3 scenario for the FF period and almost the whole country for SPEI6 and SPEI12. Compared to 1980-2014, droughts above SD are projected to occur six times more frequently in most regions. Therefore, it is quite remarkable that droughts above SD have increased to an extent in the northern region where most of the country's agriculture is located.

4.4 Variation of drought in agricultural growing seasons

In this section, the focus is brought towards the potential future occurrence of drought during the agricultural season. In Morocco, cereals are the most produced agricultural products based mainly on wheat and barely. As stated in (Karrou and Oweis, 2014), the growing season of these two products ranges roughly from November to April. First, we analize the relationship between the cereal production of Morocco obtained from the Food and Agriculture Organization (FAO), and the index values calculated for the stations in the north of the country. In Figure 7, the bars represent the normalized cereal crops (barley and wheat), and the lines indicate the mean SPEI values. Notice that for a better insight of the results, each value is normalized by its maximum. According to this figure, the variation of major cereal productions in Morocco follows closely the variation of the considered SPEI indices. The correlation coefficients between these two index values and amounts of grain production vary between 0.55 and 0.75. For example, while the correlation coefficient between the SPEI-6 (Nov-Apr) for the barley is 0.75, it is 0.66 for the wheat. This clearly demonstrates that the production of cereals in Morocco is highly impacted by drought occurrence. By assuming that

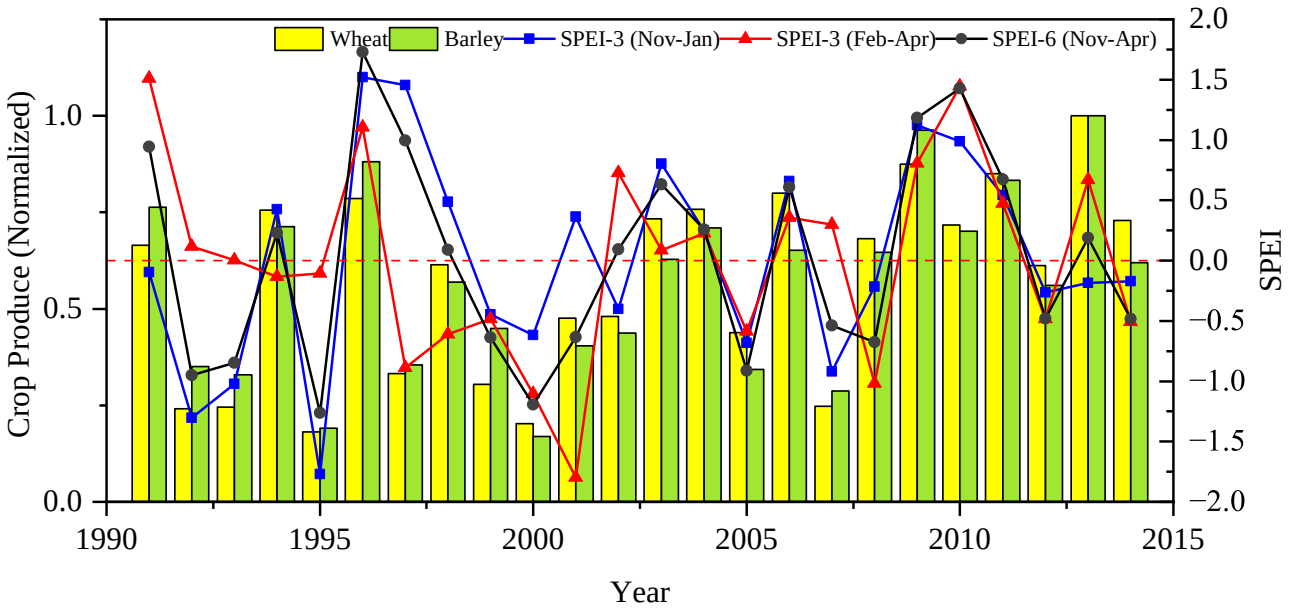

Figure 7: Relationship between SPEI indices and normalized agricultural production of Barley, Corn, and Wheat in Morocco (1991-2014).

the same agricultural practices are preserved in the future, potential changes in drought occurrence may enhance the change in the production of cereals. Therefore, the spatial distributions of the 3- and 6-month SPEI values covering the growth periods of cereal crops in Morocco for drought conditions (SPEI < 0) are displayed in Figure 8. The percentage of drought occurrence in the country between 1980-2014 is around 50%. Although according to the SSP2-4.5 scenario, drought in NF for SPEI3 (Nov-Jan) is found to increase slightly in the north-east regions, the increase is more pronounced in SPEI-3 (Feb-Apr) and SPEI-6 (Nov-Apr). Furthermore, in the SSP5-8.5 scenario, a significant increase is observed at all time scales after 2050. It is also evident that after 2075, the percentage of drought occurrence in the northern region is around 80% on average. In the context of these assessments, if the SSP5-8.5 scenario is to be realized, problems of agricultural production will inevitably arise in Morocco after the mid-century.

5 Discussions

In this study, the drought pattern of Morocco, an important country in northwest africa, is analyzed both spatially and temporally with the SPEI method using CMIP6 future projections. Temporal and spatial analyses of drought and climatic parameters are analyzed for historical (1980-2014), NF (2025-2049), MF (2050-2074), and FF (2075-2100) periods. The broad perspective of the presented study has provided the opportunity to evaluate it from different aspects with other studies in the literature. First, when changes in the precipitation, PET and aridity indexes based on the historical observation data (1980-2014) for the study area are analyzed, it is found that the PET values are in an increasing trend, while the precipitation and AI values are in a decreasing trend. In this context, the determination of an increase in the PET values and a decrease in AI values in the study conducted by (Ullah et al., 2022) on a global scale with the CRU reanalysis data sets covering the period between 1901 and 2019 is consistent with the results of the present study. The increase

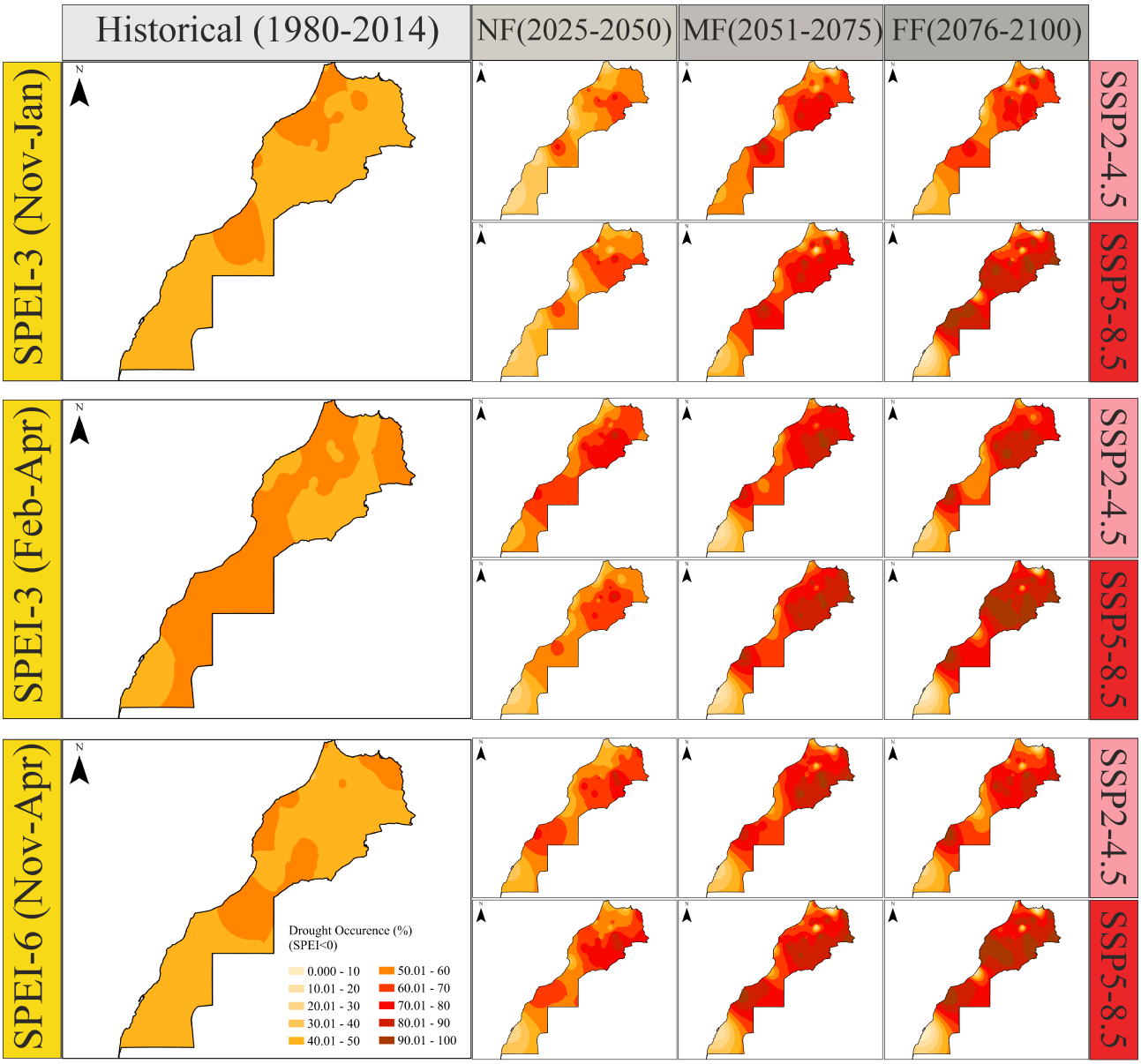

Figure 8: Spatial variation of drought in the agricultural growing seasons.

in likelihood of the drought occurrence in the country is also linked to the expected decrease in precipitation, especially in the northern region. It is worth mentioning that this latter is a dominant factor on the drought assessment. This decrease is more pronounced in the FF period especially following SSP5-8.5 scenario, and it is consistent with many previous studies in the region (El Moçayd et al., 2020; Carvalho et al., 2022; Zittis et al., 2019; Majdi et al., 2022; Spinoni et al., 2020; Li and Li, 2022; Ukkola et al., 2020). It is found that changes in the PET, which is another important parameter that affects drought, are significantly influenced mainly by changes in the temperature. Especially in the region from the atlas mountains in the northeast of the region to the Algerian border where significant increase is expected. It should be stressed that the increase in PETs, especially in this region, was also reported by (El Moçayd et al., 2020; Carvalho et al., 2022). Based on the results related to the aridity index, which is an important indicator of temporal climate regimes of the study area, the northern region according to the SSP5-8.5 scenario may not be considered as

a humid area in the future. It is predicted that the climate, which was humid and semi-humid in the historical period in the region, may change to a semi-arid and arid regime from the NF to the FF period. In addition, many regions in the country which are considered humid under the present climate situations are likely to move to arid conditions under the climate change impact, compare the results summarized in Table 4. In the far future period (2081-2100) in (Carvalho et al., 2022), especially in the northern part of the region, increases in arid areas with decreases in the AI values are clearly seen. The increase in arid areas in the northern part of the region is also stated by (Zhang et al., 2021). In another study conducted on a global scale, (Wang et al., 2020) examined changes in the precipitation, PET, and aridity index depending on two climate change scenarios. In their study, increases in the PETs and decreases in the aridity index were determined for the region in consideration according to the 2 °C warming scenarios, which are more pronounced in a range of 4 °C warming, especially in the northern region. It should be pointed out that a similar situation was also emphasized in the study by (Koutroulis, 2019).

The temporal evaluations of drought indices for different time scales (3-6-12 months) show that all drought time scales are spatially in parallel with different frequencies. As the drought time scale increases, the percentage of drought occurrence also increases. Results presented in this study demonstrate that major parts of the country are likely to be affected by the drought with an increasing severity throughout the time, and this particularly true in the SSP5-8.5 scenario. In this respect, increases in the drought frequencies and severities related to the country's northern region according to the SPEI12 scenario in the study conducted by (Spinoni et al., 2020) according to RCP2-4.5 and RCP5-8.5 scenarios only for the years 2071-2100 are important supporting this point. Authors in (Zeng et al., 2022) demonstrated that there are increases in drought severity for the region in a global scale study. Another study by (Vicente-Serrano et al., 2020) predicts that the region will face more severe drought conditions, especially in the northern part of the region, according to the SPEI-12 ≤ -1.28 threshold in a global drought assessment made according to RCP scenarios. In a global study conducted by (Spinoni et al., 2021), it was emphasized that increases in the drought frequencies and severities increase as the amount of warming increases according to the SPEI-12¡-1 threshold depending on different warming scenarios (+1.5, +2, +3, +4 °C) in the western Mediterranean. The results obtained in the presented study are in agreement with these results.

In the considered study area, the potential impact of the projected scenarios for drought occurrence on agriculture is assessed. The focus was brought to the cereal sector, which is one of the most important agricultural product industries (Achli et al., 2022) and an important part of this production is vulnerable to climate variation, especially the rain-fed cereals (which constitutes 90% of the agricultural areas). Following the inter-annual variability in Morocco, most of the precipitation in the region falls between November and April. This may probably explain the high correlation found between changes in the SPEI-3 (Nov-Feb) and the SPEI-6 (Nov-Apr) and the cereal production as depicted in Figure 7 in this study. Assuming the same agricultural practices are preserved in the future, potential changes of drought occurrence are likely to drive the change in cereal production, especially during the growing season. Accordingly, Figure 8 confirms that the increase in percentage of drought occurrence in both SPEI3 and SPEI6 scenarios between November-April, when cereal growth is the highest, will adversely affect production. Especially in the northern region where agricultural areas are dense, the increases will be higher. (Hakam et al., 2023) analyzed the relationship between values of the SPI-SPEI index and cereal crop yields in two provinces in the northwest of Morocco (2000-2020). This study shows that the change in crop yields is parallel to the seasonal humid or dry periods. In addition, in some years of the study, the SPI values in the region were more humid than the SPEI values, but the decreases in crop yields revealed that temperature is

the critical factor affecting most of the variations in cereal yields. Note that precipitation and the temperature conditions of cereal crops are particularly important during the spring-summer period of the growth and development up to the harvest period (Hakam et al., 2023). Therefore, as shown in Figure 8, increases in the percentage of drought occurrence during the SPEI (Feb-Apr) period are quite significant. It is also clear that this situation confirms that cereal production in the country may be vulnerable in the future.

6 Conclusions

In this study, potential future changes of drought occurrence under the climate change impact have been evaluated in Morocco with a focus on the main cereals growing season. First, an ANN-based MME of CMIP6's GCMs was used to carefully select the most accurate predictors and to statistically downscale the precipitation and temperature variables in the region. Those models were then used in order to predict future changes in these variables under the SSP2-4.5 and SSP5-8.5 scenarios for climate change. This allowed estimating the future changes in the PET, AI, and SPEI values and it has been found that precipitation is likely to decrease while PET values are projected to increase, leading to a significant increase in the AI values. Under the climate change impact, many regions in the country considered to be humid/sub-humid under past climate situations are likely to move to arid conditions. Next, the analysis of drought occurrence under historical conditions and climate change impact has been performed. Generally, it has been found that the country is likely to face severe drought conditions in the future. The obtained results reveal that drought severity tends to increase, and the drought occurrence above severe drought would be six times more frequent than the past conditions in most regions. Moreover, the drought analysis results during the growing season of cereal crops showed that the percentage of drought occurrence in the northern region is expected to reach around 80%. These results also suggest that climate change will surely impact crop patterns in Morocco with future projections likely to increase the occurrence of severe droughts episodes in the region. Based on the high correlation between these events and cereal production and assuming that agricultural practices are kept as in the present time, many regions in the country will not be suitable for cereal production. Ultimately, this will harshly impact food security in the country. These findings highlight the need for effective adaptation strategies to mitigate the potential impacts of drought in Morocco such as water management, crop selection, and land-use planning.

It is also recommended that future studies should focus on more detailed analyses of the impact of climate change on specific sectors such as agriculture, water resources and public health in north african countries including Morocco. This class of studies may pave the way for examining the effectiveness of different adaptation strategies including water conservation measures and crop diversification in mitigating the impacts of drought and climate change.

Author contributions

V. Gumus: Conceptualization, Software, Writing - Original Draft, Formal analysis, **N. El Moçayd:** Conceptualization, Writing - Original Draft, Validation, Resources, Data Curation, **M. Seker:** Methodology, Formal analysis, Writing - Original Draft, **M. Seaid:** Writing - Review & Editing, Validation, Visualization

Acknowledgments

The authors greatly acknowledge Dr Moulay Driss Hasnaoui from the Moroccan Water Ministry and the Moroccan State Meteorological Service in Morocco for providing the meteorological data used in this study. Additionally, the valuable comments provided by the reviewer and editor have significantly enhanced the quality of this study. Their contributions are sincerely appreciated.

Availability of data and materials

The data underlying the results can be obtained from the corresponding author on a reasonable request. Data about agricultural productivity in Morocco had been downloaded from FAOSTAT `https://www.fao.org/faostat/en/#home`

Funding

The first author has been supported by The Scientific and Research Council of Turkey (TUBITAK) to conduct research under TUBITAK-2219-International Postdoctoral Research Fellowship Program for Turkish Citizens. The second author has been supported by OCP through the UMRP program.

References

Achli, S., Epule, T. E., Dhiba, D., Chehbouni, A., and Er-Raki, S. (2022). Vulnerability of barley, maize, and wheat yields to variations in growing season precipitation in morocco. *Applied Sciences*, 12(7).

AghaKouchak, A., Mirchi, A., Madani, K., Di Baldassarre, G., Nazemi, A., Alborzi, A., Anjileli, H., Azarderakhsh, M., Chiang, F., Hassanzadeh, E., Huning, L. S., Mallakpour, I., Martinez, A., Mazdiyasni, O., Moftakhari, H., Norouzi, H., Sadegh, M., Sadeqi, D., Van Loon, A. F., and Wanders, N. (2021). Anthropogenic drought: Definition, challenges, and opportunities. *Reviews of Geophysics*, 59(2):e2019RG000683.

Ahmed, K., Sachindra, D., Shahid, S., Iqbal, Z., Nawaz, N., and Khan, N. (2020). Multi-model ensemble predictions of precipitation and temperature using machine learning algorithms. *Atmospheric Research*, 236:104806.

Anderson, W., Taylor, C., McDermid, S., Ilboudo-Nébié, E., Seager, R., Schlenker, W., Cottier, F., de Sherbinin, A., Mendeloff, D., and Markey, K. (2021). Violent conflict exacerbated drought-related food insecurity between 2009 and 2019 in sub-saharan africa. *Nature Food*, 2(8):603–615.

Begueria, S., Vicente-Serrano, S. M., Reig, F., and Latorre, B. (2014). Standardized precipitation evapotranspiration index (spei) revisited: parameter fitting, evapotranspiration models, tools, datasets and drought monitoring. *International Journal of Climatology*, 34(10):3001–3023.

Benbrahim, K. F., Ismaili, M., Benbrahim, S. F., and Tribak, A. (2004). Land degradation by desertification and deforestation in morocco. *Science et changements planétaires/Sécheresse*, 15(4):307–320.

Bi, D., Dix, M., Marsland, S., O'Farrell, S., Rashid, H., Uotila, P., Hirst, A., Kowalczyk, E., Golebiewski, M., Sullivan, A., Yan, H., Hannah, N., Franklin, C., Sun, Z., Vohralik, P., Watterson, I., Zhou, X., Fiedler, R., Collier, M., Ma, Y., Noonan, J., Stevens, L., Uhe, P., Zhu, H., Griffies, S., Hill, R., Harris, C., and Puri, K. (2013). The ACCESS coupled model: Description, control climate and evaluation. *Australian Meteorological and Oceanographic Journal*, 63(1):41–64.

Boucher, O., Servonnat, J., Albright, A. L., Aumont, O., Balkanski, Y., Bastrikov, V., Bekki, S., Bonnet, R., Bony, S., Bopp, L., Braconnot, P., Brockmann, P., Cadule, P., Caubel, A., Cheruy, F., Codron, F., Cozic, A., Cugnet, D., D'Andrea, F., Davini, P., de Lavergne, C., Denvil, S., Deshayes, J., Devilliers, M., Ducharne, A., Dufresne, J., Dupont, E., Éthé, C., Fairhead, L., Falletti, L., Flavoni, S., Foujols, M., Gardoll, S., Gastineau, G., Ghattas, J., Grandpeix, J., Guenet, B., Guez, L. E., Guilyardi, E., Guimberteau, M., Hauglustaine, D., Hourdin, F., Idelkadi, A., Joussaume, S., Kageyama, M., Khodri, M., Krinner, G., Lebas, N., Levavasseur, G., Lévy, C., Li, L., Lott, F., Lurton, T., Luyssaert, S., Madec, G., Madeleine, J., Maignan, F., Marchand, M., Marti, O., Mellul, L., Meurdesoif, Y., Mignot, J., Musat, I., Ottlé, C., Peylin, P., Planton, Y., Polcher, J., Rio, C., Rochetin, N., Rousset, C., Sepulchre, P., Sima, A., Swingedouw, D., Thiéblemont, R., Traore, A. K., Vancoppenolle, M., Vial, J., Vialard, J., Viovy, N., and Vuichard, N. (2020). Presentation and evaluation of the IPSL-CM6A-LR climate model. *Journal of Advances in Modeling Earth Systems*, 12(7).

Cao, J., Wang, B., Yang, Y.-M., Ma, L., Li, J., Sun, B., Bao, Y., He, J., Zhou, X., and Wu, L. (2018). The nuist earth system model (NESM) version 3: description and preliminary evaluation. *Geoscientific Model Development*, 11(7):2975–2993.

Carvalho, D., Pereira, S. C., Silva, R., and Rocha, A. (2022). Aridity and desertification in the mediterranean under euro-cordex future climate change scenarios. *Climatic Change*, 174(3-4).

Chaqdid, A., Tuel, A., Fatimy, A. E., and Moçayd, N. E. (2023). Extreme rainfall events in morocco: Spatial dependence and climate drivers. *Weather and Climate Extremes*, page 100556.

D'Odorico, P., Laio, F., and Ridolfi, L. (2010). Does globalization of water reduce societal resilience to drought? *Geophysical Research Letters*, 37(13).

Doukkali, M. (2005). Water institutional reforms in morocco. *Water Policy*, 7(1):71–88.

Driouech, F., Stafi, H., Khouakhi, A., Moutia, S., Badi, W., ElRhaz, K., and Chehbouni, A. (2021). Recent observed country-wide climate trends in morocco. *International Journal of Climatology*, 41:E855–E874.

Dunne, J. P., Horowitz, L. W., Adcroft, A. J., Ginoux, P., Held, I. M., John, J. G., Krasting, J. P., Malyshev, S., Naik, V., Paulot, F., Shevliakova, E., Stock, C. A., Zadeh, N., Balaji, V., Blanton, C., Dunne, K. A., Dupuis, C., Durachta, J., Dussin, R., Gauthier, P. P. G., Griffies, S. M., Guo, H., Hallberg, R. W., Harrison, M., He, J., Hurlin, W., McHugh, C., Menzel, R., Milly, P. C. D., Nikonov, S., Paynter, D. J., Ploshay, J., Radhakrishnan, A., Rand, K., Reichl, B. G., Robinson, T., Schwarzkopf, D. M., Sentman, L. T., Underwood, S., Vahlenkamp, H., Winton, M., Wittenberg, A. T., Wyman, B., Zeng, Y., and Zhao, M. (2020). The GFDL earth system model version 4.1 (GFDL-ESM 4.1): Overall coupled model description and simulation characteristics. *Journal of Advances in Modeling Earth Systems*, 12(11).

El Moçayd, N., Kang, S., and Eltahir, E. A. (2020). Climate change impacts on the water highway project in morocco. *Hydrology and Earth System Sciences*, 24(3):1467–1483.

Elalaoui, O., Fadlaoui, A., Maatala, N., and Ibrahimy, A. (2021). Agriculture and gdp causality nexus in morocco: Empirical evidence from a var approach. *International Journal of Agricultural Economics*, 6(4):198–207.

Elkharrim, M. and Bahi, L. (2015). Using statistical downscaling of gcm simulations to assess climate change impacts on drought conditions in the northwest of morocco. *Modern Applied Science*, 9(2):1.

Esper, J., Frank, D., Büntgen, U., Verstege, A., Luterbacher, J., and Xoplaki, E. (2007). Long-term drought severity variations in morocco. *Geophysical research letters*, 34(17).

Ezzine, H., Bouziane, A., and Ouazar, D. (2014). Seasonal comparisons of meteorological and agricultural drought indices in morocco using open short time-series data. *International Journal of Applied Earth Observation and Geoinformation*, 26:36–48.

Filahi, S., Tanarhte, M., Mouhir, L., El Morhit, M., and Tramblay, Y. (2016). Trends in indices of daily temperature and precipitations extremes in morocco. *Theoretical and Applied Climatology*, 124:959–972.

Fniguire, F., Laftouhi, N.-E., Saidi, M. E., Zamrane, Z., El Himer, H., and Khalil, N. (2017). Spatial and temporal analysis of the drought vulnerability and risks over eight decades in a semi-arid region (Tensift basin: Morocco). *Theoretical and Applied Climatology*, 130(1):321–330.

Gadouali, F., Semane, N., Muñoz, Á., and Messouli, M. (2020). On the link between the madden-julian oscillation, Euro-Mediterranean weather regimes, and Morocco winter rainfall. *Journal of Geophysical Research: Atmospheres*, 125(8):e2020JD032387.

Gumus, V., El Moçayd, N., Seker, M., and Seaid, M. (2023). Evaluation of future temperature and precipitation projections in morocco using the ann-based multi-model ensemble from cmip6. *Atmospheric Research*, 292:106880.

Gutjahr, O., Putrasahan, D., Lohmann, K., Jungclaus, J. H., von Storch, J.-S., Brüggemann, N., Haak, H., and Stössel, A. (2019). Max Planck institute earth system model (MPI-ESM1.2) for the high-resolution model intercomparison project (HighResMIP). *Geoscientific Model Development*, 12(7):3241–3281.

Hakam, O., Baali, A., and Belhaj Ali, A. (2023). Modeling drought-related yield losses using new geospatial technologies and machine learning approaches: case of the gharb plain, north-west morocco. *Modeling Earth Systems and Environment*, 9(1):647–667.

Ivčević, A., Bertoldo, R., Mazurek, H., Siame, L., Guignard, S., Moussa, A. B., and Bellier, O. (2020). Local risk awareness and precautionary behaviour in a multi-hazard region of north morocco. *International Journal of Disaster Risk Reduction*, 50:101724.

Kadi, M. A. (2002). Irrigation water pricing policy in morocco's large scale irrigation projects. *Hamdy, A., Lacirignola, C. Lamaddaleny, N (eds), Water valuation and cost recovery mechanisms in the developing countries of the Mediterranean region. Bari*.

Karrou, M. and Oweis, T. (2014). Assessment of the severity and impact of drought spells on rainfed cereals in morocco. *African Journal of Agricultural Research*, 9(49):3519–3530.

Kelley, M., Schmidt, G. A., Nazarenko, L. S., Bauer, S. E., Ruedy, R., Russell, G. L., Ackerman, A. S., Aleinov, I., Bauer, M., Bleck, R., Canuto, V., Cesana, G., Cheng, Y., Clune, T. L., Cook, B. I., Cruz, C. A., Del Genio, A. D., Elsaesser, G. S., Faluvegi, G., Kiang, N. Y., Kim, D., Lacis, A. A., Leboissetier, A., LeGrande, A. N., Lo, K. K., Marshall, J., Matthews, E. E., McDermid, S., Mezuman, K., Miller, R. L., Murray, L. T., Oinas, V., Orbe, C., García-Pando, C. P., Perlwitz, J. P., Puma, M. J., Rind, D., Romanou, A., Shindell, D. T., Sun, S., Tausnev, N., Tsigaridis, K., Tselioudis, G., Weng, E., Wu, J., and Yao, M. (2020). GISS-E2.1: Configurations and climatology. *Journal of Advances in Modeling Earth Systems*, 12(8).

Khomsi, K., Mahe, G., Tramblay, Y., Sinan, M., and Snoussi, M. (2016). Regional impacts of global change: seasonal trends in extreme rainfall, run-off and temperature in two contrasting regions of morocco. *Natural Hazards and Earth System Sciences*, 16(5):1079–1090.

Knippertz, P., Christoph, M., and Speth, P. (2003). Long-term precipitation variability in Morocco and the link to the large-scale circulation in recent and future climates. *Meteorology and Atmospheric physics*, 83(1):67–88.

Koutroulis, A. G. (2019). Dryland changes under different levels of global warming. *Science of The Total Environment*, 655:482–511.

Kulyamin, D. V. and Volodin, E. M. (2018). INM RAS coupled atmosphere–ionosphere general circulation model INMAIM (0–130 km). *Russian Journal of Numerical Analysis and Mathematical Modelling*, 33(6):351–357.

Le Page, M. and Zribi, M. (2019). Analysis and predictability of drought in northwest africa using optical and microwave satellite remote sensing products. *Scientific reports*, 9(1):1466.

Lee, S., Moriasi, D. N., Mehr, A. D., and Mirchi, A. (2024). Sensitivity of standardized precipitation and evapotranspiration index (spei) to the choice of spei probability distribution and evapotranspiration method. *Journal of Hydrology: Regional Studies*, 53:101761.

Li, L., She, D., Zheng, H., Lin, P., and Yang, Z.-L. (2020a). Elucidating diverse drought characteristics from two meteorological drought indices (spi and spei) in china. *Journal of Hydrometeorology*, 21(7):1513–1530.

Li, L., Yu, Y., Tang, Y., Lin, P., Xie, J., Song, M., Dong, L., Zhou, T., Liu, L., Wang, L., Pu, Y., Chen, X., Chen, L., Xie, Z., Liu, H., Zhang, L., Huang, X., Feng, T., Zheng, W., Xia, K., Liu, H., Liu, J., Wang, Y., Wang, L., Jia, B., Xie, F., Wang, B., Zhao, S., Yu, Z., Zhao, B., and Wei, J. (2020b). The flexible global ocean-atmosphere-land system model grid-point version 3 (FGOALS-g3): Description and evaluation. *Journal of Advances in Modeling Earth Systems*, 12(9).

Li, X. and Li, Z. (2022). Global water availability and its distribution under the coupled model intercomparison project phase six scenarios. *International Journal of Climatology*, 42(11):5748–5767.

Liu, X., Zhu, X., Pan, Y., Li, S., Liu, Y., and Ma, Y. (2016). Agricultural drought monitoring: Progress, challenges, and prospects. *Journal of Geographical Sciences*, 26:750–767.

Maggioni, E. (2015). Water demand management in times of drought: What matters for water conservation. *Water Resources Research*, 51(1):125–139.

Majdi, F., Hosseini, S. A., Karbalaee, A., Kaseri, M., and Marjanian, S. (2022). Future projection of precipitation and temperature changes in the middle east and north africa (mena) region based on cmip6. *Theoretical and Applied Climatology*, 147(3-4):1249–1262.

Manzanas, R., Brands, S., San-Martín, D., Lucero, A., Limbo, C., and Gutiérrez, J. (2015). Statistical downscaling in the tropics can be sensitive to reanalysis choice: a case study for precipitation in the philippines. *Journal of Climate*, 28(10):4171–4184.

McKee, T. B., Doesken, N. J., Kleist, J., et al. (1993). The relationship of drought frequency and duration to time scales. In *Proceedings of the 8th Conference on Applied Climatology*, volume 17, pages 179–183. Boston.

Middleton, N. and Thomas, D. (1992). *UNEP: World atlas of desertification*. Edward Arnold, Sevenoaks. Edward Arnold, Sevenoaks.

Ortiz-Gómez, R., Flowers-Cano, R. S., and Medina-García, G. (2022). Sensitivity of the rdi and spei drought indices to different models for estimating evapotranspiration potential in semiarid regions. *Water Resources Management*, 36(7):2471–2492.

Pour, S. H., Shahid, S., Chung, E.-S., and Wang, X.-J. (2018). Model output statistics downscaling using support vector machine for the projection of spatial and temporal changes in rainfall of bangladesh. *Atmospheric research*, 213:149–162.

Satour, N., Raji, O., El Moçayd, N., Kacimi, I., and Kassou, N. (2021). Spatialized flood resilience measurement in rapidly urbanized coastal areas with a complex semi-arid environment in northern morocco. *Natural Hazards and Earth System Sciences*, 21(3):1101–1118.

Seker, M. and Gumus, V. (2022). Projection of temperature and precipitation in the Mediterranean region through multi-model ensemble from CMIP6. *Atmospheric Research*, 280.

Spinoni, J., Barbosa, P., Bucchignani, E., Cassano, J., Cavazos, T., Cescatti, A., Christensen, J. H., Christensen, O. B., Coppola, E., Evans, J. P., Forzieri, G., Geyer, B., Giorgi, F., Jacob, D., Katzfey, J., Koenigk, T., Laprise, R., Lennard, C. J., Kurnaz, M. L., Li, D., Llopart, M., McCormick, N., Naumann, G., Nikulin, G., Ozturk, T., Panitz, H., Rocha, R. P., Solman, S. A., Syktus, J., Tangang, F., Teichmann, C., Vautard, R., Vogt, J. V., Winger, K., Zittis, G., and Dosio, A. (2021). Global exposure of population and land-use to meteorological droughts under different warming levels and ssps : A cordex -based study. *International Journal of Climatology*, 41(15):6825–6853.

Spinoni, J., Barbosa, P., Bucchignani, E., Cassano, J., Cavazos, T., Christensen, J. H., Christensen, O. B., Coppola, E., Evans, J., Geyer, B., Giorgi, F., Hadjinicolaou, P., Jacob, D., Katzfey, J., Koenigk, T., Laprise, R., Lennard, C. J., Kurnaz, M. L., Li, D., Llopart, M., McCormick, N., Naumann, G., Nikulin, G., Ozturk, T., Panitz, H.-J., Porfirio da Rocha, R., Rockel, B., Solman, S. A., Syktus, J., Tangang, F., Teichmann, C., Vautard, R., Vogt, J. V., Winger, K., Zittis, G., and Dosio, A. (2020). Future global meteorological drought hot spots: A study based on cordex data. *Journal of Climate*, 33(9):3635–3661.

Stagge, J. H., Tallaksen, L. M., Gudmundsson, L., Van Loon, A. F., and Stahl, K. (2015). Candidate distributions for climatological drought indices (spi and spei). *International Journal of Climatology*, 35(13):4027–4040.

Svoboda, M., Hayes, M., and Wood, D. (2012). Standardized precipitation index: user guide. *World Meteorological Organization Geneva, Switzerland*.

Swart, N. C., Cole, J. N. S., Kharin, V. V., Lazare, M., Scinocca, J. F., Gillett, N. P., Anstey, J., Arora, V., Christian, J. R., Hanna, S., Jiao, Y., Lee, W. G., Majaess, F., Saenko, O. A., Seiler, C., Seinen, C., Shao, A., Sigmond, M., Solheim, L., von Salzen, K., Yang, D., and Winter, B. (2019). The canadian earth system model version 5 (canESM5.0.3). *Geoscientific Model Development*, 12(11):4823–4873.

Séférian, R., Nabat, P., Michou, M., Saint-Martin, D., Voldoire, A., Colin, J., Decharme, B., Delire, C., Berthet, S., Chevallier, M., Sénési, S., Franchisteguy, L., Vial, J., Mallet, M., Joetzjer, E., Geoffroy, O., Guérémy, J., Moine, M., Msadek, R., Ribes, A., Rocher, M., Roehrig, R., Salas-y-Mélia, D., Sanchez, E., Terray, L., Valcke, S., Waldman, R., Aumont, O., Bopp, L., Deshayes, J., Éthé, C., and Madec, G. (2019). Evaluation of cnrm earth system model, cnrm-ESM2-1: Role of earth system processes in present-day and future climate. *Journal of Advances in Modeling Earth Systems*, 11(12):4182–4227.

Tardieu, F. (2020). Educated big data to study sensitivity to drought. *Nature Food*, 1(11):669–670.

Tatebe, H., Ogura, T., Nitta, T., Komuro, Y., Ogochi, K., Takemura, T., Sudo, K., Sekiguchi, M., Abe, M., Saito, F., Chikira, M., Watanabe, S., Mori, M., Hirota, N., Kawatani, Y., Mochizuki, T., Yoshimura, K., Takata, K., O'Ishi, R., Yamazaki, D., Suzuki, T., Kurogi, M., Kataoka, T.,

Watanabe, M., and Kimoto, M. (2019). Description and basic evaluation of simulated mean state, internal variability, and climate sensitivity in miroc6. *Geoscientific Model Development*, 12(7):2727–2765.

Tuel, A. (2020). *Precipitation variability and change over Morocco and the Mediterranean*. PhD thesis, Massachusetts Institute of Technology.

Tuel, A., El Moçayd, N., Hasnaoui, M. D., and Eltahir, E. A. (2022). Future projections of high atlas snowpack and runoff under climate change. *Hydrology and Earth System Sciences*, 26(3):571–588.

Tuel, A. and Eltahir, E. A. (2020). Why is the Mediterranean a climate change hot spot? *Journal of Climate*, 33(14):5829–5843.

Tuel, A., Kang, S., and Eltahir, E. A. (2021). Understanding climate change over the southwestern Mediterranean using high-resolution simulations. *Climate Dynamics*, 56:985–1001.

Ukkola, A. M., De Kauwe, M. G., Roderick, M. L., Abramowitz, G., and Pitman, A. J. (2020). Robust future changes in meteorological drought incmip6projections despite uncertainty in precipitation. *Geophysical Research Letters*, 47(11).

Ullah, S., You, Q., Sachindra, D. A., Nowosad, M., Ullah, W., Bhatti, A. S., Jin, Z., and Ali, A. (2022). Spatiotemporal changes in global aridity in terms of multiple aridity indices: An assessment based on the cru data. *Atmospheric Research*, 268.

Van Loon, A. F. (2015). Hydrological drought explained. *Wiley Interdisciplinary Reviews: Water*, 2(4):359–392.

Vicente-Serrano, S. M., Beguería, S., and López-Moreno, J. I. (2010). A multiscalar drought index sensitive to global warming: The standardized precipitation evapotranspiration index. *Journal of Climate*, 23(7):1696–1718.

Vicente-Serrano, S. M., Quiring, S. M., Peña-Gallardo, M., Yuan, S., and Domínguez-Castro, F. (2020). A review of environmental droughts: Increased risk under global warming? *Earth-Science Reviews*, 201.

Voldoire, A., Saint-Martin, D., Sénési, S., Decharme, B., Alias, A., Chevallier, M., Colin, J., Guérémy, J. F., Michou, M., Moine, M. P., Nabat, P., Roehrig, R., Salas y Mélia, D., Séférian, R., Valcke, S., Beau, I., Belamari, S., Berthet, S., Cassou, C., Cattiaux, J., Deshayes, J., Douville, H., Ethé, C., Franchistéguy, L., Geoffroy, O., Lévy, C., Madec, G., Meurdesoif, Y., Msadek, R., Ribes, A., Sanchez-Gomez, E., Terray, L., and Waldman, R. (2019). Evaluation of CMIP6 deck experiments with CNRM-CM6-1. *Journal of Advances in Modeling Earth Systems*, 11(7):2177–2213.

Wang, H., Chen, Y., Pan, Y., Chen, Z., and Ren, Z. (2019). Assessment of candidate distributions for spi/spei and sensitivity of drought to climatic variables in china. *International Journal of Climatology*, 39(11):4392–4412.

Wang, X., Jiang, D., and Lang, X. (2020). Future changes in aridity index at two and four degrees of global warming above preindustrial levels. *International Journal of Climatology*, 41(1):278–294.

Ward, F. A. and Pulido-Velazquez, M. (2008). Water conservation in irrigation can increase water use. *Proceedings of the National Academy of Sciences*, 105(47):18215–18220.

Wilhite, D. A. and Glantz, M. H. (1985). Understanding: the drought phenomenon: The role of definitions. *Water International*, 10(3):111–120.

Wyser, K., van Noije, T., Yang, S., von Hardenberg, J., O'Donnell, D., and Döscher, R. (2020). On the increased climate sensitivity in the ec-earth model from cmip5 to cmip6. *Geoscientific Model Development*, 13(8):3465–3474.

Yu, H., Zhang, Q., Wei, Y., Liu, C., Ren, Y., Yue, P., and Zhou, J. (2022). Bias-corrections on aridity index simulations of climate models by observational constraints. *International Journal of Climatology*, 42(2):889–907.

Yukimoto, S., Kawai, H., Koshiro, T., Oshima, N., Yoshida, K., Urakawa, S., Tsujino, H., Deushi, M., Tanaka, T., Hosaka, M., Yabu, S., Yoshimura, H., Shindo, E., Mizuta, R., Obata, A., Adachi, Y., and Ishii, M. (2019). The meteorological research institute earth system model version 2.0, MRI-ESM2.0: Description and basic evaluation of the physical component. *Journal of the Meteorological Society of Japan. Ser. II*, 97(5):931–965.

Zeng, J., Li, J., Lu, X., Wei, Z., Shangguan, W., Zhang, S., Dai, Y., and Zhang, S. (2022). Assessment of global meteorological, hydrological and agricultural drought under future warming based on cmip6. *Atmospheric and Oceanic Science Letters*, 15(1).

Zhang, C., Yang, Y., Yang, D., and Wu, X. (2021). Multidimensional assessment of global dryland changes under future warming in climate projections. *Journal of Hydrology*, 592.

Zittis, G., Hadjinicolaou, P., Klangidou, M., Proestos, Y., and Lelieveld, J. (2019). A multi-model, multi-scenario, and multi-domain analysis of regional climate projections for the mediterranean. *Regional Environmental Change*, 19(8):2621–2635.